

On the sodium overabundance of giants in open clusters: The case of the Hyades^{*}

Rodolfo Smiljanic[†]

European Southern Observatory, Karl-Schwarzschild-Str. 2, 85748 Garching bei München, Germany

Accepted . Received ; in original form

ABSTRACT

Sodium abundances have been determined in a large number of giants of open clusters but conflicting results, ranging from solar values to overabundances of up to five orders of magnitude, have been found. The reasons for this disagreement are not well-understood. As these Na overabundances can be the result of deep mixing, their proper understanding has consequences for models of stellar evolution. As discussed in the literature, part of this disagreement comes from the adoption of different corrections for non-LTE effects and from the use of different atomic data for the same set of lines. However, a clear picture of the Na behaviour in giants is still missing. To contribute in this direction, this work presents a careful redetermination of the Na abundances of the Hyades giants, motivated by the recent measurement of their angular diameters. An average of $[\text{Na}/\text{Fe}] = +0.30$, in NLTE, has been found. This overabundance can be explained by hydrodynamical models with high initial rotation velocities. This result, and a trend of increasing Na with increasing stellar mass found in a previous work, suggests that there is no strong evidence of Na overabundances in red giants beyond those values expected by evolutionary models of stars with more than $\sim 2 M_{\odot}$.

Key words: open clusters and associations: individual: Hyades – stars: abundances – stars: evolution – stars: fundamental parameters.

1 INTRODUCTION

In many stages of their evolution, low- and intermediate-mass stars show signs of mixing between material of the surface with material of the interior that has been processed by nuclear reactions (Pinsonneault 1997; Charbonnel & Talon 2008; Smiljanic et al. 2009, and references therein).

The standard model of stellar evolution, where convection is the only mixing mechanism, does not account for all the observational details. The introduction of non-standard physical processes, such as atomic diffusion, rotation-induced mixing, internal gravity waves, magnetic buoyancy and thermohaline mixing, is unavoidable (see e.g. Montalbán & Schatzman 2000; Young et al. 2003; Talon & Charbonnel 2005; Palacios et al. 2006; Denissenkov & Pinsonneault 2008; Denissenkov et al. 2009; Charbonnel & Lagarde 2010; Michaud et al. 2004, 2010; Angelou et al. 2011; Palmerini et al. 2011, and references therein).

As a star leaves the main sequence towards the red giant branch (RGB), its convective envelope deepens, causing first a dilution of lithium, beryllium, and boron (Lèbre et al. 1999; Pasquini et al. 2004; Smiljanic et al. 2010; Canto Martins et al. 2011) and then the first dredge-up (Iben 1967), when material affected by hydrogen burning is mixed to the surface. The dredge-up causes an increase of the abundance of nitrogen and a decrease of carbon and of the $^{12}\text{C}/^{13}\text{C}$ ratio (Charbonnel et al. 1998; Gratton et al. 2000).

An extensive literature has shown a further modification of the surface abundances after the bump in the luminosity function on the RGB. At this phase the abundances of Li, C and the ratio $^{12}\text{C}/^{13}\text{C}$ are further decreased while that of N increases. This effect has been detected in stars of the field and of both open and globular clusters (see e.g. Sneden et al. 1986; Gilroy 1989; Gilroy & Brown 1991; Charbonnel et al. 1998; Gratton et al. 2000; Tautvaišienė et al. 2000, 2005, 2010; Smith et al. 2002; Pavlenko et al. 2003; Pilachowski et al. 2003; Geisler et al. 2005; Spite et al. 2006; Recio-Blanco & de Laverny 2007; Smiljanic et al. 2009; Mikolaitis et al. 2010, 2011; Suda et al. 2011, and references therein).

^{*} Based on data obtained from the ESO Science Archive Facility. The observations were made with ESO Telescopes at the La Silla Paranal Observatory under programmes ID 070.D-0421, 072.C-0393, and 083.A-9011.

[†] E-mail: rsmiljan@eso.org

1.1 The case of sodium

During the first dredge-up, Na produced by the NeNa-cycle (Denisenkov & Denisenkova 1990) in H-burning regions can potentially be mixed to the surface. The observational behaviour of this element, however, is not clear. In open clusters, stars with Na overabundances as high as $[\text{Na}/\text{Fe}]^1 = +0.50$ or more have been reported (Bragaglia et al. 2001; Friel et al. 2003; Jacobson et al. 2007; Schuler et al. 2009), while others were found to have mild overabundances of $[\text{Na}/\text{Fe}] \sim +0.20$ (Hamdani et al. 2000; Tautvaišienė et al. 2000; Pasquini et al. 2004; Friel et al. 2010) or abundances close to solar (Randich et al. 2006; Sestito et al. 2007; Smiljanic et al. 2009; Pancino et al. 2010).

One of the factors behind this discrepancy is the adoption of different $\log gfs$ for the same Na lines by different authors. For example, the $\log gfs$ adopted in Smiljanic et al. (2009), from the NIST database (Ralchenko et al. 2010), are on average 0.22 dex higher than those adopted by Jacobson et al. (2007), derived with respect to Arcturus. Indeed, as discussed later by Jacobson et al. (2008), a revision of their gf -values resulted in an increase of about 0.20 dex with corresponding decrease in the Na abundances. The use of this revised scale now results in modest overabundances, $[\text{Na}/\text{Fe}] = +0.10 \dots +0.20$ (see Table 14 of Friel et al. 2010) in comparison with the strong overabundances found in Jacobson et al. (2007), $[\text{Na}/\text{Fe}] = +0.40 \dots +0.60$.

Another issue are departures from the local thermodynamic equilibrium (LTE). Several authors provide non-LTE corrections for Na (Baumueller et al. 1998; Gratton et al. 1999; Mashonkina et al. 2000; Takeda et al. 2003; Shi et al. 2004; Andrievsky et al. 2007; Lind et al. 2011). As discussed by Lind et al. (2011), there is a scatter of 0.10 to 0.20 dex among the different corrections. Usually non-LTE abundances are smaller than the LTE ones.

In the abundance analyses cited above, the different authors made different choices regarding these matters. It is thus difficult to make sense out of these results and understand whether there is a real problem with the sodium overabundances in giants. Dedicated studies aiming to better understand this issue are still lacking in the literature.

The re-analysis of Na in the Hyades giants presented here is a step on this direction. It is motivated by the recent determination of angular diameters (and thus fundamental effective temperatures – T_{eff}) for the four Hyades giants from interferometric measurements using the CHARA array by Boyajian et al. (2009). Accurate Na abundances can help clarifying whether the strong overabundances are real and test whether there is an offset between observations and evolutionary models.

This paper is divided as follows. Section 2 presents the observational data used in the analysis and the determination of the atmospheric parameters of the Hyades giants. Section 3 presents the determination of Na abundance from equivalent widths and spectrum synthesis while Sec. 4 presents a discussion of the results. Section 5 summarizes the conclusions.

2 THE HYADES

The Hyades are the closest open cluster to the Sun (~ 46.5 pc, van Leeuwen 2009). They have an age of 625 ± 50 Myr (Perryman et al. 1998) and a metallicity of $[\text{Fe}/\text{H}] = +0.13 \pm 0.01$ (Paulson et al. 2003). There is no sign of Na overabundance in the dwarf stars, i.e. $[\text{Na}/\text{Fe}] \sim 0.00$ (Paulson et al. 2003). For the giants an average of $[\text{Na}/\text{Fe}] = +0.48$ (in LTE) was found by Schuler et al. (2009), which the authors regard as “too large to be explained by any known self-enrichment scenario”.

The cluster has four evolved members, all He-burning clump giants: ϵ Tau (HR 1409 or HD 28305), γ Tau (HR 1346 or HD 27371), δ^1 Tau (HR 1373 or HD 27697), and θ^1 Tau (HR 1411 or HD 28307). A fifth suggested giant member, δ Ari (HR 951) is likely a non-member (de Bruijne et al. 2001). The stars ϵ Tau and γ Tau are single stars while δ^1 Tau and θ^1 are spectroscopic binaries (Griffin et al. 1988; Mermilliod et al. 2008). In addition, the star ϵ Tau was found to have a massive planetary companion (Sato et al. 2007).

An HR diagram of the Hyades on the region around the turn-off and the clump is shown in Fig. 1. An isochrone from Girardi et al. (2002) with 625 Myr and $[\text{Fe}/\text{H}] = +0.13$ indicates that a clump giant in the Hyades has $\sim 2.48 M_{\odot}$. To illustrate, the corresponding isochrone is also shown in Fig. 1 (no attempt to find the best fitting model was made).

2.1 Observational data

High-resolution spectra of three Hyades giants obtained with FEROS (Kaufer et al. 1999) at the 2.2m MPG/ESO telescope at La Silla and with UVES (Dekker et al. 2000) fed by the UT2 of the VLT at Paranal are analyzed here.

FEROS is a fiber-fed echelle spectrograph that provides a full wavelength coverage of $\lambda\lambda 350\text{--}920$ nm over 39 orders at $R = 48\,000$. The spectra were reduced using the FEROS Data Reduction System (DRS) as implemented within ESO-MIDAS. UVES is a cross-dispersed echelle spectrograph able to obtain spectra from the atmospheric cut-off at 300 nm to ~ 1100 nm. Reduction was done with the ESO UVES pipeline within MIDAS (Ballester et al. 2000).

The FEROS data of stars δ^1 Tau and γ Tau were made available to the author by Luca Pasquini (2010, private communication). The FEROS spectra of ϵ Tau and the UVES spectra of ϵ Tau and δ^1 Tau were retrieved from the ESO/ST-ECF science archive facility. The log book of the observations is given in Table 1.

2.2 Effective temperatures

As the only giants of the nearest open cluster, these stars have been analyzed many times. To obtain an idea of the range of temperatures found in the literature, previous determinations of the effective temperature (T_{eff}) of the four giants were queried at the PASTEL catalogue (Soubiran et al. 2010).

A few selected and recent results, together with a “literature average”, are given in Table 2 along with the corresponding reference. Note that the T_{eff} calculated with the interferometric data by Boyajian et al. (2009) is not included in the PASTEL catalogue.

¹ $[\text{A}/\text{B}] = \log [\text{N}(\text{A})/\text{N}(\text{B})]_{\star} - \log [\text{N}(\text{A})/\text{N}(\text{B})]_{\odot}$

Table 1. Observational data.

Star	Spectrograph	V	Date of observation	Exp. Time (s)	S/N @ 617 nm
γ Tau	FEROS	3.654	05 Mar. 2004	120	500
ϵ Tau	FEROS	3.540	03 Oct. 2009	180	500
	UVES RED 580		30 Nov. 2002	2×1	400
δ^1 Tau	FEROS	3.764	31 Oct. 2000	120	700
	UVES RED 580		30 Nov. 2002	2×1	250

Table 2. Effective temperatures of the Hyades giants taken from selected recent works from the literature.

Star	T_{eff} (K)	Method	Reference
γ Tau	4844 ± 47	Interferometry	Boyajian et al. (2009)
	4965 ± 75	IRFM ¹	Schuler et al. (2009)
	4960 ± 8.1	Line-depth ratio (average)	Kovtyukh et al. (2006)
	4981 ± 80	Average	Selected results from the PASTEL catalogue
δ^1 Tau	4826 ± 51	Interferometry	Boyajian et al. (2009)
	4938 ± 75	IRFM ¹	Schuler et al. (2009)
	4975 ± 7.6	Line-depth ratio (average)	Kovtyukh et al. (2006)
	5000 ± 80	FeI excitation equilibrium	Hekker & Meléndez (2007)
	4968 ± 82	Average	Selected results from the PASTEL catalogue
ϵ Tau	4827 ± 44	Interferometry	Boyajian et al. (2009)
	4911 ± 75	IRFM ¹	Schuler et al. (2009)
	4925 ± 8.7	Line-depth ratio (average)	Kovtyukh et al. (2006)
	4910 ± 80	FeI excitation equilibrium	Hekker & Meléndez (2007)
	4925 ± 84	Average	Selected results from the PASTEL catalogue

(1) The effective temperatures adopted by Schuler et al. (2009) were calculated by Blackwell & Lynas-Gray (1994) using the infrared flux method for γ and δ^1 Tau and by Blackwell & Lynas-Gray (1998) for ϵ Tau.

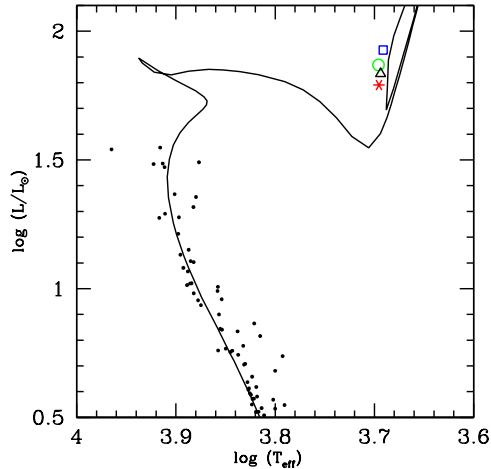


Figure 1. HR diagram of the Hyades on the region around the turn-off and the clump. The four giants are shown with different symbols (ϵ Tau as the blue square, γ Tau as the green circle, δ^1 Tau as the black triangle, and θ^1 Tau as the red star). Luminosities and temperatures are from de Bruijne et al. (2001).

There is a range of about 300–350 K on the values of T_{eff} determined for each star. As discussed in Boyajian et al. (2009), the values determined from recent angular diameters are on the low side of this range. Similarly, using the angular diameter of the Li-rich giant HD148 193, Baines et al. (2011)

derived an T_{eff} that is on the cooler side of the range of temperatures determined in the literature. Together these results might be indicating that the temperature of giants is usually overestimated.

In the following discussion, Na abundances are calculated using two values of temperature for each star: The interferometric temperatures of Boyajian et al. (2009) and those used by Schuler et al. (2009) in their abundance analysis of the same stars. The temperatures of Schuler et al. (2009) are close to the average literature values (see Table 2) and differ from the interferometric ones by 90 to 150 K.

2.3 Gravities

Gravities for the Hyades giants were determined with the equation:

$$\log(g_*/g_\odot) = \log(M_*/M_\odot) + 4 \log(T_{\text{eff}*}/T_{\text{eff}\odot}) - \log(L_*/L_\odot)$$

The luminosities by de Bruijne et al. (2001), a mass of $2.48 M_\odot$, and the usual solar values ($T_{\text{eff}\odot} = 5777$ K and $\log g_\odot = 4.44$) were adopted. For consistency, gravities were calculated using each of the T_{eff} adopted for the analysis. In addition, to illustrate the effect of the gravity in the Na abundance, additional values were determined for γ Tau assuming masses of 2.0 and $3.0 M_\odot$. It can be seen that this change in the mass causes only a minor change on $\log g$, arguing that this parameter is well constrained for these stars.

Table 3. The different sets of atmospheric parameters calculated for the Hyades giants.

Star	T_{eff}	$\log g$	[Fe/H]	Note
γ Tau	4844	2.66	$+0.14 \pm 0.05$	Interferometric T_{eff}
	4844	2.57	$+0.13 \pm 0.05$	As above with $2.0 M_{\odot}$
	4844	2.74	$+0.15 \pm 0.05$	As above with $3.0 M_{\odot}$
	4965	2.70	$+0.23 \pm 0.05$	IRFM T_{eff}
δ^1 Tau	4826	2.69	$+0.18 \pm 0.06$	Interferometric T_{eff}
	4938	2.73	$+0.25 \pm 0.06$	IRFM T_{eff}
ϵ Tau	4827	2.60	$+0.26 \pm 0.08$	Interferometric T_{eff}
	4911	2.63	$+0.31 \pm 0.08$	IRFM T_{eff}

2.4 Microturbulence

Throughout the analysis, a fixed value of microturbulence, $\xi = 1.30 \text{ km s}^{-1}$ was always adopted. This is a typical value found for the giants analyzed in Smiljanic et al. (2009). This value was checked against empirical relations from the literature that calibrate ξ as a function of $\log g$ and/or T_{eff} . Five calibrations from four references were investigated. It is interesting to note that some of these calibrations are given only as a function of $\log g$:

- (i) $\xi = 2.22 - 0.322 \log g$ (Gratton et al. 1996, derived from giants with [Fe/H] between -1.00 to 0.00),
- (ii) $\xi = 1.5 - 0.13 \log g$ (Carretta et al. 2004, derived from open cluster giants with [Fe/H] between -0.37 to $+0.24$),
- (iii) $\xi = 1.645 + (3.854 \times 10^{-4} (T_{\text{eff}} - 6387)) + (-0.64 (\log g - 4.373)) + (-3.427 \times 10^{-4} (T_{\text{eff}} - 6387) (\log g - 4.373))$ (Allende Prieto et al. 2004, derived from solar neighborhood stars with [Fe/H] between -0.50 to $+0.50$),
- (iv) $\xi = 3.40 - 4.41 \times 10^{-4} T_{\text{eff}}$ and $\xi = 1.84 - 0.202 \log g$ (Alves-Brito et al. 2010, derived from bulge, thin and thick disc giants with [Fe/H] between -1.50 to $+0.50$).

The values obtained from these calibrations for γ Tau are given in Table 4 for the parameters using the interferometric and IRFM temperatures. All these calibrations, apart from that of Carretta et al. (2004) give values that are very close to the one adopted here. What is more important, they show that the variation in T_{eff} within the range considered here does not result in a large change in microturbulence. This argues that the choice of keeping ξ constant does not introduce systematic effects in the current analysis.

2.5 Metallicity

To estimate the metallicity of the stars ([Fe/H]), equivalent widths of a set of 15 selected Fe I lines were measured. The line list, atomic data, and equivalent widths are given in Table 5. The C_6 broadening constants were taken from Coelho et al. (2005). The adopted solar iron abundance is $A(\text{Fe}) = 7.50$ (Grevesse & Sauval 1998). Using the interferometric temperatures, the mean metallicity of the Hyades giants is found to be $[\text{Fe}/\text{H}] = +0.19 \pm 0.06$. Using the IRFM temperatures, this value increases to $[\text{Fe}/\text{H}] = +0.26 \pm 0.04$.

Table 4. Microturbulence velocities (in km s^{-1}) derived with different calibrations for γ Tau, using both the interferometric and the IRFM temperature and the corresponding $\log g$.

Calibration	Interf. T_{eff}	IRFM T_{eff}
Gratton et al. (1996)	1.37	1.35
Allende Prieto et al. (2004)	1.24	1.35
Carretta et al. (2004)	1.15	1.15
Alves-Brito et al. (2010) – T_{eff}	1.26	1.25
Alves-Brito et al. (2010) – $\log g$	1.30	1.29

3 SODIUM ABUNDANCES

3.1 Line selection and atomic data

All the 32 strong NaI and NaII lines with wavelengths between 4000 and 8200 Å listed by Sansonetti & Martin (2005) were considered as possible features to be used in this analysis. The profiles of these lines were checked both in the UVES² and the Kurucz (2005) solar spectra and in the spectrum of γ Tau. All lines that were heavily blended or too strong for an abundance analysis were discarded (e.g. lines at λ 8183 and λ 8194 Å). The atomic data of the remaining NaI lines are listed in Table 6. The excitation potential and the $\log gf$ of the lines were adopted from the NIST database (Ralchenko et al. 2010). The C_6 broadening constants were adopted from Coelho et al. (2005) and Barbuy et al. (2006). An assessment of each line is given below:

- (1) 5148.838 Å: In the solar spectra the line has $\sim 14 \text{ mÅ}$. It is slightly blended on the blue wing with a line of similar strength. In the γ Tau spectrum the two lines are completely blended but their bottoms can be distinguished. Only possible to analyze with spectrum synthesis.
- (2) 5682.633 Å: It is clear in the solar spectra that the blue wing is blended with a weaker line. In the spectrum of γ Tau the blend can not be recognized, but the line is asymmetric. Equivalent widths would be affected by the blend and thus spectrum synthesis should be preferred. In the Sun the line has $\sim 100 \text{ mÅ}$.
- (3) 5688.193 & 5688.205 Å: These lines are the fine structure components of the same transition. The feature is strong in the Sun ($\gtrsim 120 \text{ mÅ}$) and stronger in γ Tau ($\gtrsim 170 \text{ mÅ}$). Seems to be clean enough, but it is too strong for an analysis using equivalent widths.
- (4) 6154.226 Å: On the Sun there is a weak line close to the red wing at $\sim 6154.43 \text{ Å}$. On γ Tau the same blend is apparent but less distinguishable. There is another weak line at $\sim 6154.6 \text{ Å}$. The line seems to deviate from a Gaussian profile towards a Voigt one already in the Sun (where $\text{EW} \sim 37 \text{ mÅ}$). Analysis using equivalent widths should be possible.
- (5) 6160.747 Å: Both in the Sun and in γ Tau, the placement of the continuum is affected by the wing of the strong nearby CaI 6162.2 Å line. It has closeby lines to the blue and red sides, but the profile seems clean. Analysis using equivalent widths is possible. It has $\sim 60 \text{ mÅ}$ in the Sun.

² The spectrum is available for download at the ESO website: www.eso.org/observing/dfo/quality/UVES/pipeline/solar_spectrum.html

Table 5. Atomic data and equivalent widths of the Fe I lines used to derive the metallicity of the stars.

λ (Å)	χ (eV)	log gf	C_6	Sun (mÅ)	γ Tau (mÅ)	δ^1 Tau (mÅ)	ϵ Tau (mÅ)
5054.642	3.64	-2.032	4.68E-32	40.2	80.6	80.2	84.5
5127.679	0.05	-6.005	7.38E-33	22.3	96.6	99.5	105.6
5223.185	3.64	-2.285	6.00E-32	29.7	65.8	68.8	76.0
5320.035	3.64	-2.542	8.91E-32	19.8	57.1	57.9	59.0
5483.098	4.15	-1.481	2.95E-31	46.5	78.8	80.8	83.1
5522.446	4.21	-1.432	3.02E-31	43.6	78.5	80.6	83.8
5778.453	2.59	-3.524	4.95E-32	22.2	73.6	74.6	81.1
5784.658	3.40	-2.626	3.57E-31	27.2	67.8	70.7	76.2
5814.807	4.28	-1.861	2.82E-31	23.4	56.5	58.1	59.7
6012.209	2.22	-3.843	3.35E-32	24.2	78.7	78.4	82.3
6079.008	4.65	-1.055	5.13E-31	46.2	77.8	80.9	81.2
6187.989	3.94	-1.712	4.90E-31	47.9	91.2	93.1	99.6
6271.278	3.33	-2.797	2.78E-31	23.6	68.3	74.2	79.5
6739.522	1.56	-4.942	2.10E-32	11.8	63.6	64.8	70.3
6837.006	4.59	-1.756	2.46E-32	17.5	47.1	50.2	52.1

Table 6. Atomic data of the six selected NaI lines.

λ (Å)	log gf	χ (eV)	C_6
5 148.838	-2.044	2.102	1.01E-30
5 682.633	-0.706	2.102	3.38E-30
5 688.193*	-1.406	2.104	2.03E-30
5 688.205*	-0.452	2.104	3.38E-30
6 154.226	-1.547	2.102	0.90E-31
6 160.747	-1.246	2.104	0.30E-31

(*) Fine structure components.

3.2 Equivalent widths

Given the above assessment, only the equivalent widths of the lines at 6154 and 6160 Å were used to determine Na abundances. However, other lines have been used in the literature. For example, Schuler et al. (2009) also use the line at 5682 Å, which is clearly blended in the Sun and is asymmetric in γ Tau. The equivalent width of such line should be regarded as suspicious. Indeed, from the three lines adopted by Schuler et al. (2009), line 5682 Å always results in an abundance that is higher by 0.10–0.14 dex than that obtained with the lines at 6154 and 6160 Å. Without this line, the mean [Na/Fe] for the Hyades giants found by Schuler et al. (2009) is reduced by 0.05 dex.

Equivalent widths were determined by fitting Gaussian profiles to the observed lines using IRAF³. For the Sun, lines were measured both in the UVES and in the Kurucz spectrum. The values obtained are listed in Table 7.

Model atmospheres were computed using the Linux version (Sbordone et al. 2004; Sbordone 2005) of the ATLAS9 code originally developed by Kurucz (see e.g. Kurucz 1993). For the calculations, the opacity distribution functions of Castelli & Kurucz (2003) without overshooting were adopted. These models assume local thermodynamic equilib-

rium, plane-parallel geometry, and hydrostatic equilibrium. Abundances were derived using the WIDTH code, also in its Linux version. For the Hyades giants, abundances were calculated only with the equivalent widths measured in the FEROS spectra, as they have higher S/N. These Na abundances are listed in Table 8.

3.3 Spectrum synthesis

Abundances were also derived using spectrum synthesis and all the Na lines in Table 6. Synthetic spectra were calculated with the codes described in Coelho et al. (2005) and the model atmospheres described above. The line list is the one used to compute the spectrum library of Coelho et al. (2005). As mentioned before, the Na line at 5682 Å is blended in its blue wing. In the line list used here, this blend is due to a Cr I line at 5682.495 Å, with log $gf = -0.609$. It was modeled with the solar abundance recommended by Grevesse & Sauval (1998), $A(\text{Cr})_{\odot} = 5.67$. The Na abundances obtained with spectrum synthesis are listed in Table 9.

3.4 Uncertainties of the Na abundances

The main source of error of the abundances are the errors of the atmospheric parameters. The uncertainty of the T_{eff} derived by Boyajian et al. (2009) is of the order of ± 50 K. This corresponds to an average uncertainty of ± 0.04 dex in the Na abundance – $A(\text{Na})$ – and ± 0.03 in [Fe/H].

As shown for γ Tau (Table 3), gravities are well constrained and no significant impact on the Na abundance is expected. A change of ± 0.05 dex in log g results in a change of ∓ 0.015 dex in $A(\text{Na})$. The same uncertainty causes an effect of ∓ 0.005 in [Fe/H].

The discussion in Section 2.4 shows that the value of ξ is well constrained. The values given by the different calibrations have an rms of ± 0.08 km s⁻¹. A total change of ± 0.10 km s⁻¹ in ξ results in a change of ∓ 0.03 dex in $A(\text{Na})$. This change causes no significant effect in [Fe/H].

Considering that there is no significant uncertainty in

³ IRAF is distributed by the National Optical Astronomy Observatory, which is operated by the Association of Universities for Research in Astronomy, Inc., under cooperative agreement with the National Science Foundation.

Table 7. Equivalent widths of three NaI lines measured from the data collected in this work.

Line	Sun	Sun	γ Tau	δ^1 Tau	δ^1 Tau	ϵ Tau	ϵ Tau
(Å)	Kurucz	UVES	FEROS	FEROS	UVES	FEROS	UVES
(mÅ)	(mÅ)	(mÅ)	(mÅ)	(mÅ)	(mÅ)	(mÅ)	(mÅ)
6154	37.9	37.7	105.4	104.1	103.1	108.0	107.4
6160	58.1	58.6	119.6	122.8	119.8	127.0	124.8

Table 8. Sodium abundances calculated with equivalent widths and the different atmospheric parameters of each star.

Line	Sun	Sun	γ Tau	γ Tau	γ Tau	γ Tau	δ^1 Tau	δ^1 Tau	ϵ Tau	ϵ Tau
(Å)	Kurucz	UVES	Interf.	IRFM	2.0 M $_{\odot}$	3.0 M $_{\odot}$	Interf.	IRFM	Interf.	IRFM
6154	6.27	6.27	6.86	6.96	6.86	6.86	6.83	6.92	6.91	6.98
6160	6.32	6.33	6.81	6.92	6.81	6.81	6.86	6.96	6.95	7.02
Average	6.29	6.30	6.84	6.94	6.84	6.84	6.85	6.94	6.93	7.00
[Na/Fe]	–	–	+0.40	+0.41	+0.41	+0.39	+0.37	+0.39	+0.37	+0.39

the Na and Fe abundances of the Sun, the final uncertainty in [Na/Fe] is of ± 0.04 dex.

4 DISCUSSION

The mean solar abundance using equivalent widths is $A(\text{Na})_{\odot} = 6.30$ while using spectrum synthesis it is $A(\text{Na})_{\odot} = 6.33$. The average [Na/Fe] values for each star are given in Tables 8 and 9, respectively for the cases using equivalent widths and spectrum synthesis. Although there is some difference in $A(\text{Na})$ between the different temperature scales, there is basically no noticeable effect on [Na/Fe].

However, at first glance the average values determined with equivalent widths seem to be about ~ 0.12 dex higher than the values determined using spectrum synthesis. The difference is apparent in the giants but not in the Sun.

As discussed below, this is not directly related to the use equivalent widths or spectrum synthesis to derive the abundances, but to the different choice of lines used in each case. There is however, a systematic difference of about ~ 0.10 dex between the abundances derived with the λ 6154 line. This likely comes from an uncertainty in the equivalent width of this line. An error on the equivalent width of $\pm 6\text{mÅ}$ can produce a change of ± 0.10 on the abundance.

There are three effects contributing to the difference. One, is the Na abundance given by the λ 5148 line. Excluding it from the average, the [Na/Fe] values increase by ~ 0.05 dex. It is not clear why this line results systematically in smaller values. Nevertheless, it was decided to consider its abundance as suspicious and to exclude it from further discussion. The final average LTE [Na/Fe] values, without line λ 5148, are given in Table 10. A second effect discussed in the next subsection are the NLTE corrections.

The last effect seems related to differences between the WIDTH code, used to calculate abundances from equivalent widths, and the PFANT code, used to compute the synthetic spectrum.

Following a suggestion by the referee, a series of synthetic spectra with the parameters of γ Tau at the region around the line λ 6160 were calculated with different Na abundances. The equivalent widths were measured and the

values used to recompute the abundances. The resulting Na abundances given by WIDTH are 0.03 to 0.04 dex higher than the values used to compute the synthetic spectra.

At this point, it is not possible to say whether this is caused by some numerical effect, by some difference in other input data (e.g. partition functions, opacities...), or to some difference in the physics, like the treatment of broadening, for example. This should, of course, be further investigated. Nevertheless, as it is based in the analysis of more features and likely based in a more reliable way to deal with the effects of broadening, the abundances derived with spectrum synthesis are preferred here.

4.1 NLTE abundances

As mentioned in the introduction, the Na lines are affected by NLTE effects (see Lind et al. 2011, and references therein). This has been suggested as a likely reason behind the large Na overabundances found in giants of open clusters (see e.g. Randich et al. 2006; Sestito et al. 2007).

To correct the abundances calculated here, the NLTE calculations of Lind et al. (2011) were adopted. Corrections were interpolated among the grid calculated in that work with an IDL routine kindly made available to the author by Karin Lind (2011, private communication). NLTE corrections were derived in a line-by-line basis, giving as input the atmospheric parameters and the LTE abundances⁴.

Individual line corrections for all stars (giants and Sun) range from -0.03 (for line 5148 Å) up to -0.15 (for line 6160 Å). For the Sun, the average corrections are of -0.08 and -0.09 dex, respectively with the abundances using equivalent widths and spectrum synthesis. Thus, in NLTE, the solar Na abundances derived in this work are $A(\text{Na})_{\odot} = 6.22$

⁴ Alternatively, the interpolation code can accept as input the equivalent width of the line and return both the LTE and the NLTE abundances. The first approach was preferred here because the LTE abundances calculated in Lind et al. (2011) for a given set of atmospheric parameters are slightly different from the ones derived in this work. The difference is caused by different choices made in the treatment of line broadening.

Table 9. Sodium abundances with spectrum synthesis and the different atmospheric parameters of each star.

Line (Å)	Sun Kurucz	Sun UVES	γ Tau Interf.	γ Tau IRFM	δ^1 Tau Interf.	δ^1 Tau IRFM	ϵ Tau Interf.	ϵ Tau IRFM
5148	6.24	6.24	6.48	6.56	6.49	6.58	6.53	6.62
5682	6.36	6.36	6.87	6.97	6.82	6.92	6.94	7.00
5688	6.42	6.42	6.88	6.98	6.83	6.94	6.98	7.05
6154	6.30	6.30	6.75	6.86	6.73	6.83	6.80	6.88
6160	6.32	6.32	6.81	6.91	6.85	6.96	6.93	7.00
Average [Na/Fe]	6.33 –	6.33 –	6.76 +0.29	6.86 +0.30	6.74 +0.23	6.85 +0.27	6.84 +0.25	6.91 +0.27

Table 10. Average [Na/Fe], in LTE, for each star and for each of the different analysis and parameters (excluding line λ 5148 for the synthesis values).

Analysis	γ Tau	δ^1 Tau	ϵ Tau
EqW & Interf.	+0.40	+0.37	+0.37
EqW & IRFM	+0.41	+0.39	+0.39
Synthesis & Interf	+0.34	+0.28	+0.30
Synthesis & IRFM	+0.35	+0.31	+0.32

with equivalent widths and $A(\text{Na})_{\odot} = 6.24$ with spectrum synthesis. For the giants, the different selection of lines results on average corrections of -0.14 when using equivalent widths and around -0.11 when using spectrum synthesis.

This difference in the average the NLTE corrections is another responsible for the difference among the LTE [Na/Fe] values given by equivalent widths and spectrum synthesis. With respect to the Sun, the correction when using equivalent widths (only lines 6154 and 6160 Å) is of ~ -0.06 dex. When using spectrum synthesis (4 lines), the correction is of -0.01 or -0.02 dex. This helps to explain why the different NLTE abundances in Table 11 are in better agreement than the LTE values in Table 10.

The average absolute NLTE Na abundance of the Hyades giants, using the interferometric temperatures, is found to be $[\text{Na/Fe}] = +0.30^5$. With the IRFM adopted by Schuler et al. (2009) the value found here is $[\text{Na/Fe}] = +0.31^6$.

Using equivalent widths, Schuler et al. (2009) obtained $[\text{Na/Fe}] = +0.48$ in LTE. The question then is why the results are different. First, as pointed out in Section 3.2, Schuler et al. (2009) used the equivalent width of line λ 5682 to determine the Na abundance. This line, however, is blended and removing it from the average reduces [Na/Fe] by 0.05 dex. Second are the NLTE corrections for lines λ 6154 and 6160, causing another reduction by 0.05/0.06 dex. Last, Schuler et al. (2009) adopted $[\text{Fe/H}] = +0.13$ for the Hyades giants. The atmospheric parameters used in Schuler et al. (2009) were determined in a previous paper, Schuler et al. (2006), where FeI lines were also measured. Using these lines, Schuler et al. (2006) found an average of $[\text{Fe/H}] = +0.16$, although recalculating it with the Kurucz model atmospheres and codes used here a value of $[\text{Fe/H}]$

Table 11. Average [Na/Fe] in NLTE.

Analysis	γ Tau	δ^1 Tau	ϵ Tau
EqW & Interf.	+0.34	+0.33	+0.32
EqW & IRFM	+0.35	+0.33	+0.34
Synthesis & Interf	+0.33	+0.27	+0.29
Synthesis & IRFM	+0.33	+0.29	+0.31

$= +0.19$ is found. Taking into account this difference the final [Na/Fe] in NLTE found by Schuler et al. (2009) should be $[\text{Na/Fe}] = +0.34$ (in the Schuler et al. 2006, metallicity scale) or $[\text{Na/Fe}] = +0.31$ (in the metallicity scale recalculated here). These values are in perfect agreement with the ones derived in this work.

4.2 Comparison with evolutionary models

An interesting question to look at now is whether the Na overabundances of the Hyades giants can be explained by evolutionary models. In standard models, no modification of the Na abundance is expected after the first dredge-up for stars below $\sim 2.0 M_{\odot}$ (Mowlavi 1999; Charbonnel & Lagarde 2010). For stars of higher mass, an increase of up to $+0.20$ dex in the Na abundance is expected.

When mixing induced by rotation is included in the models (transport of chemicals and angular momentum by shear turbulence and meridional circulation), larger overabundances are produced. These effects can also create a dispersion in the Na abundance among otherwise similar stars if they had different initial rotation velocities in the zero age main sequence (Charbonnel & Lagarde 2010). This happens because rotation affects the internal abundance profile of the elements involved in H-burning. In this way, the Na-rich region in rotating stars begins further out from the core, and more Na-rich material can be dredged-up to the surface.

In Fig. 2 the Na abundance of the Hyades is shown in comparison with the models calculated by Charbonnel & Lagarde (2010). Also shown in the figure are the Na abundances of 31 giants of 10 open clusters derived in Smiljanic et al. (2009). These clusters have turn-off masses between 1.7 and $3.1 M_{\odot}$. The recommended Na abundance of the Hyades ($[\text{Na/Fe}] = +0.30$) is in the upper part of the range expected by the models. Therefore, and contrary to the conclusion of Schuler et al. (2009), this comparison shows that the Na abundance in the Hyades can be explained by modern hydrodynamical models that include the effects

⁵ Using equivalent widths the value is $[\text{Na/Fe}] = +0.33$.

⁶ Using equivalent widths the value is $[\text{Na/Fe}] = +0.34$.

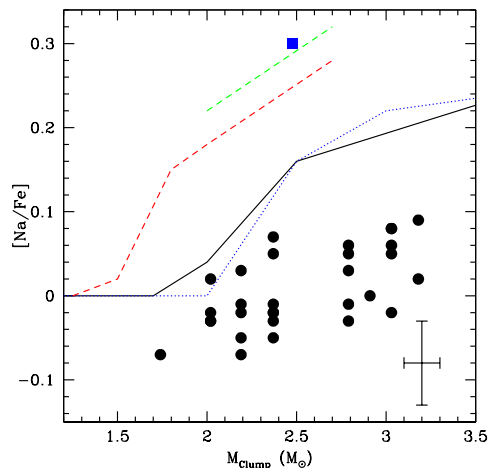


Figure 2. Sodium abundances, $[\text{Na}/\text{Fe}]$, as function of the stellar mass at the clump. The circles indicate the open cluster giants analyzed in Smiljanic et al. (2009), the typical error bar of that work is shown in the lower right corner. The blue square corresponds to the recommended $[\text{Na}/\text{Fe}]$ of the Hyades derived in this work. The lines represent the predicted $[\text{Na}/\text{Fe}]$ as a function of initial stellar mass given by the models of Charbonnel & Lagarde (2010) for the standard case (solid line), for a model including thermohaline mixing only (blue dotted line), and models with thermohaline mixing and rotation-induced mixing with initial velocities in the ZAMS of 250 and 300 km s^{-1} (lower red dashed line and upper green dashed line, respectively).

of rotation. There is no need for an extra unknown mixing process.

Although it is believed here that the absolute Na abundance of the Hyades was derived, this claim can not be extended to most of the results in the literature. One way to avoid such systematics and test whether the Na overabundances in giants conform with the prediction of the models, is to conduct a large homogeneous analysis of a sample including only giants but with different masses. In this way one can look for abundance trends with mass and test if they agree with the expectations of models.

This is exemplified by the giants analyzed in Smiljanic et al. (2009). As seen in Fig. 2 and discussed also in Smiljanic et al. (2009) and Charbonnel & Lagarde (2010), there is an off-set of about 0.10 dex between observations and models. However, there is an agreement in the increasing trend with mass. This suggests that we are indeed observing the effects of mixing in these stars, in spite of a possible systematic effect in the abundance scale.

The Na abundance of the Hyades derived here and the trend of increasing Na with increasing mass found in Smiljanic et al. (2009) argue that there is no strong evidence for overabundances above those expected by the models, for stars above $2 M_{\odot}$.

At this point, it is interesting to mention the results of Pasquini et al. (2004) for the cluster IC 4651 and of Randich et al. (2006) for M67. Pasquini et al. (2004) found a systematic difference at the level of 0.20 dex between the Na abundances of dwarfs and giants in IC 4651. A similar difference between dwarfs and giants was, however, not detected in stars of M67 by Randich et al. (2006). Although these results could be regarded as contradictory at first sight, they

are not. Clump giants in M67 have $\sim 1.3 M_{\odot}$ while clump giants in IC 4651 have $\sim 1.8 M_{\odot}$. As can be seen in Fig. 2, according to the models of Charbonnel & Lagarde (2010) a star of $1.3 M_{\odot}$ is never expected to enrich itself in Na after the first dredge-up while stars of $1.8 M_{\odot}$ could be enriched by $\sim +0.15$ dex. Although caution is needed in the comparison among dwarfs and giants, these results seem to support the idea that models with rotation can properly explain the behaviour of Na also in giants below $2 M_{\odot}$.

4.3 Cluster versus field giants

It is sometimes noticed that the overabundance of Na seen in giants of open clusters is not apparent in field stars (Friel 2006). This comparison is, however, usually made between giants in clusters and field dwarfs (see e.g. Jacobson et al. 2011). As also discussed by these authors, such an offset might be real and caused by mixing. Based on the discussion of the previous Section, this is a conclusion supported here. Jacobson et al. (2011) noticed indeed that their cluster abundances agree well with the Na abundances of field clump giants determined by Mishenina et al. (2006).

Comparisons among dwarfs and giants need to be careful not just because of mixing, but also because systematic effects can cause biases that might be mistaken by real differences. As an example, according to Meléndez et al. (2008) and Alves-Brito et al. (2010) this seems to be the case behind previous claims of abundance differences among thick disc and bulge stars.

A mismatch of Na abundances between stars in open clusters and in the field lead de Silva et al. (2009) to suggest that the dissolution of open clusters might not be the main contributor of stars for the Galactic disc. These authors compiled Na abundances in cluster giants from the literature, normalized them to a common solar scale, and did a comparison with Na abundances in field dwarfs from Soubiran & Girard (2005), field clump giants from Mishenina et al. (2006), and bulge giants from Fulbright, McWilliam & Rich (2007). Agreement was found between the cluster giants and the field giants of Mishenina et al. (2006), but an offset exists with respect to the dwarfs of Soubiran & Girard (2005) and the giants of Fulbright et al. (2007).

Because of mixing, an offset between Na in giants and dwarfs might be expected, with the caveat that in samples of field stars one is adding together stars with different masses and metallicities, properties that affect the mixing of Na during the first dredge-up. In other words, depending on the mass range of the giants an offset between the Na abundances between giants and dwarfs and among giants themselves might be expected or not. A robust way to attempt a comparison such as the one done by de Silva et al. (2009) would be using dwarfs in the field and dwarfs in clusters, where mixing is not able to affect the Na abundances.

5 SUMMARY

Sodium abundances of three Hyades giants have been re-determined and an average value of $[\text{Na}/\text{Fe}] = +0.30$ in NLTE was found. This Na abundance was derived using the ab-

solute T_{eff} of the stars determined with the interferometric angular diameter measurements of Boyajian et al. (2009).

This Na abundance agrees well with the ones predicted by the hydrodynamical models of Charbonnel & Lagarde (2010) for a star of $2.48 M_{\odot}$, after the first dredge-up, and taking into account rotation-induced mixing. This contradicts the conclusion of Schuler et al. (2009) that the Na overabundances of the Hyades could not be explained by any known mixing mechanism. The Na abundance of the Hyades giants are on the upper-limit of the range predicted by the models, implying that the stars had a rather high initial rotation.

Absolute abundance values have always to be considered with care. Nevertheless, as a fundamental temperature was used, the Na abundance derived here should be quite accurate. In general, relative comparisons should be more robust. In this sense, the increasing trend of the Na abundance with increasing mass found in the giants analyzed by Smiljanic et al. (2009) is the same as the one expected by evolutionary models. Agreement with models is also seen in the results of Randich et al. (2006), that did not find a difference in Na among dwarfs and giants of M67 and in the results of Pasquini et al. (2004), that did find a difference in Na among dwarfs and giants of IC 4651. In addition, it should be noticed that when comparing field giants with cluster giants, similar Na overabundances are apparent (Mishenina et al. 2006).

All these pieces of evidence seem to point to the conclusion that, so far, there seems to be no strong evidence for Na overabundances in giants of open clusters beyond those that can be well explained by the effects of evolutionary mixing, in stars more massive than $\sim 2.0 M_{\odot}$. A consistent and homogeneous reanalysis of Na abundances in a large sample of giants is still necessary to confirm (or refute) this conclusion.

ACKNOWLEDGMENTS

I thank the anonymous referee for the valuable suggestions and comments. I am also grateful to Luca Pasquini for making available the FEROS spectra of the Hyades giants and to Karin Lind for making available the code to interpolate among the grid of NLTE corrections. The research leading to these results has received funding from the European Community's Seventh Framework Programme (FP7/2007-2013) under grant agreement No 229517. This research has made use of the WEBDA database, operated at the Institute for Astronomy of the University of Vienna, of the Simbad database operated at CDS, Strasbourg, France, and of NASA's Astrophysics Data System.

REFERENCES

Allende Prieto C., Barklem P. S., Lambert D. L., Cunha K., 2004, *A&A*, 420, 183
 Alves-Brito A., Meléndez J., Asplund M., Ramírez I., Yong D., 2010, *A&A*, 513, A35+
 Andrievsky S. M., Spite M., Korotin S. A., Spite F., Bonifacio P., Cayrel R., Hill V., François P., 2007, *A&A*, 464, 1081

Angelou G. C., Church R. P., Stancliffe R. J., Lattanzio J. C., Smith G. H., 2011, *ApJ*, 728, 79
 Baines E. K., McAlister H. A., ten Brummelaar T. A., Turner N. H., Sturmann J., Sturmann L., Goldfinger P. J., Farrington C. D., Ridgway S. T., 2011, *ApJ*, 731, 132
 Ballester P., Modigliani A., Boitquin O., Cristiani S., Hanuschik R., Kaufer A., Wolf S., 2000, *The Messenger*, 101, 31
 Barbuy B., Zoccali M., Ortolani S., Momany Y., Minniti D., Hill V., Renzini A., Rich R. M., Bica E., Pasquini L., Yadav R. K. S., 2006, *A&A*, 449, 349
 Baummueller D., Butler K., Gehren T., 1998, *A&A*, 338, 637
 Blackwell D. E., Lynas-Gray A. E., 1994, *A&A*, 282, 899
 Blackwell D. E., Lynas-Gray A. E., 1998, *A&AS*, 129, 505
 Boyajian T. S., McAlister H. A., Cantrell J. R., Gies D. R., Brummelaar T. A. t., Farrington C., Goldfinger P. J., Sturmann L., Sturmann J., Turner N. H., Ridgway S., 2009, *ApJ*, 691, 1243
 Bragaglia A., Carretta E., Gratton R. G., Tosi M., Bonanno G., Bruno P., Calì A., Claudi R., Cosentino R., Desidera S., Farinato G., Rebescini M., Scuderi S., 2001, *AJ*, 121, 327
 Canto Martins B. L., Lèbre A., Palacios A., de Laverny P., Richard O., Melo C. H. F., Do Nascimento Jr. J. D., de Medeiros J. R., 2011, *A&A*, 527, A94+
 Carretta E., Bragaglia A., Gratton R. G., Tosi M., 2004, *A&A*, 422, 951
 Castelli F., Kurucz R. L., 2003, in Piskunov N., Weiss W. W., Gray D. F., eds, *Proceedings of the IAU Symposium 210: Modelling of Stellar Atmospheres New Grids of ATLAS9 Model Atmospheres Modelling of Stellar Atmospheres*. ASP, San Francisco, p. A20
 Charbonnel C., Brown J. A., Wallerstein G., 1998, *A&A*, 332, 204
 Charbonnel C., Lagarde N., 2010, *A&A*, 522, A10+
 Charbonnel C., Talon S., 2008, in Deng L., Chan K. L., eds, *Proceedings of the IAU Symposium 252 Deep inside low-mass stars*. pp 163–174
 Coelho P., Barbuy B., Meléndez J., Schiavon R. P., Castilho B. V., 2005, *A&A*, 443, 735
 de Bruijne J. H. J., Hoogerwerf R., de Zeeuw P. T., 2001, *A&A*, 367, 111
 de Silva G. M., Gibson B. K., Lattanzio J., Asplund M., 2009, *A&A*, 500, L25
 Dekker H., D’Odorico S., Kaufer A., Delabre B., Kotzlowski H., 2000, in Iye M., Moorwood A. F., eds, *Proc. SPIE, Optical and IR Telescope Instrumentation and Detectors Vol. 4008, Design, construction, and performance of UVES, the echelle spectrograph for the UT2 Kueyen Telescope at the ESO Paranal Observatory*. SPIE, pp 534–545
 Denisenkov P. A., Denisenkova S. N., 1990, *Soviet Astronomy Letters*, 16, 275
 Denissenkov P. A., Pinsonneault M., 2008, *ApJ*, 684, 626
 Denissenkov P. A., Pinsonneault M., MacGregor K. B., 2009, *ApJ*, 696, 1823
 Friel E. D., 2006, in Randich S., Pasquini L., eds, *Chemical Abundances and Mixing in Stars in the Milky Way and its Satellites, ESO Astrophysics Symposia Metallicities and α -Abundances in Open Clusters*. p. 3
 Friel E. D., Jacobson H. R., Barrett E., Fullton L., Balachandran S. C., Pilachowski C. A., 2003, *AJ*, 126, 2372

- Friel E. D., Jacobson H. R., Pilachowski C. A., 2010, *AJ*, 139, 1942
- Fulbright J. P., McWilliam A., Rich R. M., 2007, *ApJ*, 661, 1152
- Geisler D., Smith V. V., Wallerstein G., Gonzalez G., Charbonnel C., 2005, *AJ*, 129, 1428
- Gilroy K. K., 1989, *ApJ*, 347, 835
- Gilroy K. K., Brown J. A., 1991, *ApJ*, 371, 578
- Girardi L., Bertelli G., Bressan A., Chiosi C., Groenewegen M. A. T., Marigo P., Salasnich B., Weiss A., 2002, *A&A*, 391, 195
- Gratton R. G., Carretta E., Castelli F., 1996, *A&A*, 314, 191
- Gratton R. G., Carretta E., Eriksson K., Gustafsson B., 1999, *A&A*, 350, 955
- Gratton R. G., Sneden C., Carretta E., Bragaglia A., 2000, *A&A*, 354, 169
- Grevesse N., Sauval A. J., 1998, *Space Science Reviews*, 85, 161
- Griffin R. F., Griffin R. E. M., Gunn J. E., Zimmerman B. A., 1988, *AJ*, 96, 172
- Hamdani S., North P., Mowlavi N., Raboud D., Mermilliod J.-C., 2000, *A&A*, 360, 509
- Hekker S., Meléndez J., 2007, *A&A*, 475, 1003
- Iben I. J., 1967, *ApJ*, 147, 624
- Jacobson H. R., Friel E. D., Pilachowski C. A., 2007, *AJ*, 134, 1216
- Jacobson H. R., Friel E. D., Pilachowski C. A., 2008, *AJ*, 135, 2341
- Jacobson H. R., Friel E. D., Pilachowski C. A., 2011, *AJ*, 141, 58
- Kaufer A., Stahl O., Tubbesing S., Norregaard P., Avila G., Francois P., Pasquini L., Pizzella A., 1999, *The Messenger*, 95, 8
- Kovtyukh V. V., Soubiran C., Bienaymé O., Mishenina T. V., Belik S. I., 2006, *MNRAS*, 371, 879
- Kurucz R., 1993, *ATLAS9 Stellar Atmosphere Programs and 2 km/s grid*. CD-ROM No. 13. Cambridge, Mass.: Smithsonian Astrophysical Observatory.
- Kurucz R. L., 2005, *Memorie della Societa Astronomica Italiana Supplementi*, 8, 189
- Lèbre A., de Laverny P., De Medeiros J. R., Charbonnel C., da Silva L., 1999, *A&A*, 345, 936
- Lind K., Asplund M., Barklem P. S., Belyaev A. K., 2011, *A&A*, 528, A103+
- Mashonkina L. I., Shimanskii V. V., Sakhibullin N. A., 2000, *Astronomy Reports*, 44, 790
- Meléndez J., Asplund M., Alves-Brito A., Cunha K., Barbuy B., Bessell M. S., Chiappini C., Freeman K. C., Ramírez I., Smith V. V., Yong D., 2008, *A&A*, 484, L21
- Mermilliod J. C., Mayor M., Udry S., 2008, *A&A*, 485, 303
- Michaud G., Richard O., Richer J., Vandenberg D. A., 2004, *ApJ*, 606, 452
- Michaud G., Richer J., Richard O., 2010, *A&A*, 510, A104
- Mikolaitis Š., Tautvaišienė G., Gratton R., Bragaglia A., Carretta E., 2010, *MNRAS*, 407, 1866
- Mikolaitis Š., Tautvaišienė G., Gratton R., Bragaglia A., Carretta E., 2011, *MNRAS*, 413, 2199
- Mishenina T. V., Bienaymé O., Gorbaneva T. I., Charbonnel C., Soubiran C., Korotin S. A., Kovtyukh V. V., 2006, *A&A*, 456, 1109
- Montalbán J., Schatzman E., 2000, *A&A*, 354, 943
- Mowlavi N., 1999, *A&A*, 350, 73
- Palacios A., Charbonnel C., Talon S., Siess L., 2006, *A&A*, 453, 261
- Palmerini S., La Cognata M., Cristallo S., Busso M., 2011, *ApJ*, 729, 3
- Pancino E., Carrera R., Rossetti E., Gallart C., 2010, *A&A*, 511, A56+
- Pasquini L., Randich S., Zoccali M., Hill V., Charbonnel C., Nordström B., 2004, *A&A*, 424, 951
- Paulson D. B., Sneden C., Cochran W. D., 2003, *AJ*, 125, 3185
- Pavlenko Y. V., Jones H. R. A., Longmore A. J., 2003, *MNRAS*, 345, 311
- Perryman M. A. C., Brown A. G. A., Lebreton Y., Gomez A., Turon C., de Strobel G. C., Mermilliod J. C., Robichon N., Kovalevsky J., Crifo F., 1998, *A&A*, 331, 81
- Pilachowski C., Sneden C., Freeland E., Casperson J., 2003, *AJ*, 125, 794
- Pinsonneault M., 1997, *ARA&A*, 35, 557
- Ralchenko Y., Kramida A., Reader J., NIST ASD Team 2010, *NIST Atomic Database (version 4.0)*. National Institute of Standards and Technology, <http://physics.nist.gov/asd>
- Randich S., Sestito P., Primas F., Pallavicini R., Pasquini L., 2006, *A&A*, 450, 557
- Recio-Blanco A., de Laverny P., 2007, *A&A*, 461, L13
- Sansonetti J. E., Martin W. C., 2005, *J. Phys. Chem. ref. Data*, 34, 559+
- Sato B., Izumiura H., Toyota E., Kambe E., Takeda Y., Masuda S., Omiya M., Murata D., Itoh Y., Ando H., Yoshida M., Ikoma M., Kokubo E., Ida S., 2007, *ApJ*, 661, 527
- Sbordone L., 2005, *Memorie della Societa Astronomica Italiana Supplement*, 8, 61
- Sbordone L., Bonifacio P., Castelli F., Kurucz R. L., 2004, *Memorie della Societa Astronomica Italiana Supplement*, 5, 93
- Schuler S. C., Hatzes A. P., King J. R., Kürster M., The L.-S., 2006, *AJ*, 131, 1057
- Schuler S. C., King J. R., The L.-S., 2009, *ApJ*, 701, 837
- Sestito P., Randich S., Bragaglia A., 2007, *A&A*, 465, 185
- Shi J. R., Gehren T., Zhao G., 2004, *A&A*, 423, 683
- Smiljanic R., Gauderon R., North P., Barbuy B., Charbonnel C., Mowlavi N., 2009, *A&A*, 502, 267
- Smiljanic R., Pasquini L., Charbonnel C., Lagarde N., 2010, *A&A*, 510, A50
- Smith V. V., Hinkle K. H., Cunha K., Plez B., Lambert D. L., Pilachowski C. A., Barbuy B., Meléndez J., Balachandran S., Bessell M. S., Geisler D. P., Hesser J. E., Winge C., 2002, *AJ*, 124, 3241
- Sneden C., Pilachowski C. A., Vandenberg D. A., 1986, *ApJ*, 311, 826
- Soubiran C., Girard P., 2005, *A&A*, 438, 139
- Soubiran C., Le Campion J., Cayrel de Strobel G., Caylo A., 2010, *A&A*, 515, A111+
- Spite M., Cayrel R., Hill V., Spite F., François P., Plez B., Bonifacio P., Molaro P., Depagne E., Andersen J., Barbuy B., Beers T. C., Nordström B., Primas F., 2006, *A&A*, 455, 291
- Suda T., Yamada S., Katsuta Y., Komiya Y., Ishizuka C., Aoki W., Fujimoto M. Y., 2011, *MNRAS*, 412, 843
- Takeda Y., Zhao G., Takada-Hidai M., Chen Y.-Q., Saito Y.-J., Zhang H.-W., 2003, *Chinese Journal of Astronomy*

- and Astrophysics, 3, 316
Talon S., Charbonnel C., 2005, A&A, 440, 981
Tautvaišienė G., Edvardsson B., Pužeras E., Barisevičius G., Ilyin I., 2010, MNRAS, 409, 1213
Tautvaišienė G., Edvardsson B., Pužeras E., Ilyin I., 2005, A&A, 431, 933
Tautvaišienė G., Edvardsson B., Tuominen I., Ilyin I., 2000, A&A, 360, 499
van Leeuwen F., 2009, A&A, 497, 209
Young P. A., Knierman K. A., Rigby J. R., Arnett D., 2003, ApJ, 595, 1114